Published in final edited form as:
Nat Astron. 2020 ; 2020: . doi:10.1038/s41550-020-01274-z.

Meteoritic Evidence for a Ceres-sized Water-rich Carbonaceous Chondrite Parent Asteroid

V. E. Hamilton[*,1], **C. A. Goodrich**[2], **A. H. Treiman**[2], **H. C. Connolly Jr.**[3,4,5], **M. E. Zolensky**[6], **M. H. Shaddad**[7]

[1]Department of Space Studies, Southwest Research Institute, 1050 Walnut St., #300, Boulder, CO 80302 USA

[2]Lunar and Planetary Institute, Universities Space Research Association, 3600 Bay Area Blvd., Houston, TX 77058 USA

[3]Department of Geology, School of Earth and Environment, Rowan University, Glassboro, NJ 08028 USA

[4]Lunar and Planetary Laboratory, University of Arizona, Tucson, AZ 85721 USA

[5]Department of Earth and Planetary Science, American Museum of Natural History, Central Park West at 79th St., New York, NY 10024

[6]Astromaterials Research and Exploration Science, NASA Johnson Space Center, Houston, Texas 77058, USA

[7]Physics Department, University of Khartoum, Khartoum 11115, Sudan

Abstract

Carbonaceous chondrite meteorites record the earliest stages of Solar System geo-logical activities and provide insight into their parent bodies' histories. Some carbonaceous chondrites are volumetrically dominated by hydrated minerals, providing evidence for low temperature and pressure aqueous alteration[1]. Others are dominated by anhydrous minerals and textures that indicate high temperature metamorphism in the absence of aqueous fluids[1]. Evidence of hydrous metamorphism at intermediate pressures and temperatures in carbonaceous chondrite parent bodies has been virtually absent. Here we show that an ungrouped, aqueously altered carbonaceous chondrite fragment (numbered 202) from the Almahata Sitta (AhS) meteorite contains an assemblage of minerals, including amphibole, that reflect fluid-assisted metamorphism

[*]Corresponding author: hamilton@boulder.swri.edu.

Author Contributions

VEH conducted and analyzed the spectral measurements, contributed to the scientific interpretation, and coordinated and wrote the manuscript. CAG conducted and analyzed SEM and EMPA measurements, performed the parent body size modeling, and contributed to the scientific interpretation of all data. AHT contributed to the metamorphic mineral assemblage modeling and textural interpretations. HCC contributed to the scientific interpretation of the observed EPMA, textural, and spectral results. MEZ conducted EMPA and TEM measurements and contributed to the scientific interpretation of those data. MHS provided the sample of AhS 202 from the University of Khartoum collection.

Data Availability

The data shown in this paper are available from the corresponding author upon reasonable request.

Competing Interests

The authors declare no competing interests.

at intermediate temperatures and pressures on the parent asteroid. Amphiboles are rare in carbonaceous chondrites, having only been identified previously as a trace component in Allende ($CV3_{oxA}$) chondrules[2]. Formation of these minerals requires prolonged metamorphism in a large (~640–1800 km diameter), unknown asteroid. Because Allende and AhS 202 represent different asteroidal parent bodies, intermediate conditions may have been more widespread in the early Solar System than recognized from known carbonaceous chondrite meteorites, which are likely a biased sampling.

The Almahata Sitta (AhS) meteorite is an anomalous polymict ureilite, and the first meteorite fall recovered from an observed asteroid, 2008 TC_3[3–6]. Polymict ureilites represent near-surface regolith and/or daughter bodies of a ureilitic asteroid(s). They commonly contain fragments of other meteorite types, indicating the incorporation of material from different parent bodies in the early Solar System[6,7]. Some of these fragments are types of carbonaceous chondrite (CC) material, all unlike any hand samples in our collection[8,9]. The same can be said for AhS 202 (Fig. 1), a fragment from the University of Khartoum collection[4] that has been recognized as a unique CC with relatively abundant magnetite[9–11]. It is classified as an ungrouped C chondrite with oxygen isotope ratios most similar to CM and CR chondrites[9].

We have used infrared microspectroscopy (μ-FTIR), electron microprobe analysis (EMPA), and transmission electron microscopy (TEM) to characterize the mineralogy of AhS 202. Minerals typically present in aqueously altered CC meteorites include serpentine (two types), olivine, magnetite, and Fe-Ni sulfides (Supplementary Table 1). In the course of identifying minerals in μ-FTIR spectra of the matrix, chondrules, and altered chondrules, we observed silicate spectral signatures that included features not consistent with the typically dominant silicates in CC meteorites. Comparison of these signatures with terrestrial mineral reference spectra[12] allowed us to unambiguously identify them as diagnostic of the calcic amphibole tremolite, a hydrated mineral not previously identified in aqueously altered CC (Fig. 2a)[13]. EMPA analysis shows that the mineral is near-endmember tremolite (Supplementary Table 2 and Methods). Other minerals associated with hydrothermal processing, identified spectrally and/or chemically, include clinochlore (a chlorite) and diopside pyroxene (Fig. 3 and Supplementary Table 1). We have modeled the modal mineralogy of AhS 202 from its average infrared spectrum (Fig. 2b and Methods) and the retrieved vol% abundances are: phyllosilicate (serpentine + clinochlore) = 80±<1%, amphibole (tremolite) = 10±<1%, oxide (magnetite) = 6±<1%, and olivine = 4±<1% (diopside is <1 vol% and sulfides are not spectrally active in this region). This is a minimum tremolite abundance, as the matrix phyllosilicate spectra used in the model likely also include a small amount of tremolite, based on backscattered electron (BSE) imaging. The average infrared spectrum of AhS 202 broadly resembles those of the most aqueously altered CC meteorites[14], but is not well matched by any specific meteorite or meteorite group. As another means of comparison, we attempted to model the average spectrum of AhS 202 with a library of 102 CC meteorite spectra representing all petrologic types across the CI, CM, CR, CO, CV, CK, and CB groups as well as several ungrouped meteorites. The model fit to the AhS 202 spectrum (not shown) was comprised of seven CI, CM1, CR1, CM2, and ungrouped meteorites, reflecting the general spectral characteristics of an

aqueously altered, phyllosilicate-dominated meteorite. However, some of the modeled band depths and positions are not good matches to AhS 202 and the derived abundances of the modeled compositions have large uncertainties. This result further demonstrates that AhS 202 is mineralogically distinct from known CC meteorites.

The minerals identified in this work, their quantities, and their textural relationships have important implications for the parent asteroid of AhS 202. On Earth, tremolite forms at temperatures several hundred degrees Celsius higher than typical aqueously altered carbonaceous chondrites are inferred to have experienced (<~150° C)[13], providing one piece of evidence for previously unrecognized conditions on a CC parent asteroid. Textural relationships in multiple locations (Fig. 3) suggest that diopside, clinochlore, and tremolite are all alteration products of what were once type I (FeO-poor) chondrules. Specifically, type I chondrule olivine was converted to serpentine, some mesostasis (the last formed interstitial material between the larger mineral grains) was altered to form clinochlore, and some mesostasis was heated at low temperatures to produce the calcic pyroxene diopside. The diopside was then replaced by tremolite as pressure and temperature (P/T) conditions increased. The tremolite crystals and clusters can be quite large (~50–100 μm long and 10s of μm wide), suggesting a prolonged period of growth. We also identified some areas of serpentine in the AhS 202 matrix as chrysotile (Supplementary Figure 1); the microstructure (layer spacing) of this mineral is near-ideal and indicates formation over a substantial period of time not far from equilibrium conditions. Several characteristic metamorphic minerals are not present in AhS 202, at μ-FTIR, EMPA, and TEM scales. These absent minerals include talc, brucite, enstatite, carbonate, and Fe-metal.

In terrestrial geology, the alteration of rocks at elevated P/T is represented by the concept of metamorphic facies. Different facies are distinguished by mineral assemblages that form under similar P/T conditions. Boundaries between facies are gradational and relatively wide. Aqueously altered CC meteorites are not considered to be metamorphic rocks, but some have been (re-)heated[15,16] and would fall into the low pressure (<2 kbar), moderate temperature (~250 – 800°C) hornfels facies. Thermally metamorphosed CC meteorites of the CV and CK groups have experienced temperatures from ~250°C to upwards of 900°C[17,18], and also would fall into the terrestrial hornfels facies (again, they are not described as such because their pre-cursors are not typical terrestrial rocks). On the other hand, the presence of tremolite and clinochlore at the abundances observed in AhS 202 is most consistent with greenschist facies metamorphism of ultramafic rocks (see Methods), which represents intermediate pressure (~2–8 kbar) and moderate temperature (~300 – 500°C) conditions.

The abundance of tremolite amphibole is the most significant and unique characteristic of AhS 202. Similar abundances of amphibole (10 – 15 vol%) have been identified previously only in the R chondrites LaPaz Icefield (LAP) 04840 (ferri-magnesiohornblende) and Miller Range (MIL) 11207 (edenite)[19,20], where they are inferred to represent metamorphism on a disrupted and reassembled R chondrite parent body. Although some CI, CM, and CV meteorites have been heated to temperatures as high as 700°C, lack of fluid resulted in dehydration of phyllosilicates and precluded formation of abundant amphibole[16,18]. The only prior detection of amphibole in a CC meteorite is that of Brearley[2], who identified

magnesio-hornblende in the Allende meteorite ($CV3_{oxA}$). The identification of amphibole (and talc) in Allende required the use of high-resolution, transmission electron microscopy (HRTEM) to observe the minerals, which occur primarily in 0.2 μm-wide veins or small inclusions in chondrules — i.e., very small volumetric quantities. Brearley interpreted his observations as being the result of retrograde metamorphism.

Our compositional, abundance, and textural results from AhS 202 suggest that it experienced a more pervasive and potentially longer-lived period of metamorphism than suggested by the Allende occurrence. We consider three basic scenarios for the alteration history of AhS 202: impact heating, prograde metamorphism, and retrograde metamorphism. We eliminate impact heating based on the lack of any shock textures as well as evidence for a prolonged period of metamorphism. A few relict chondrules are elongated, but this characteristic is not uniquely attributable to impact processes. Our observations of exceptionally well-formed chrysotile serpentine in the matrix of AhS 202 (Supplementary Figure 1), along with the significant abundances of the relatively high P/T minerals tremolite (many in the form of large, euhedral crystals) and clinochlore lead us to favor prograde over retrograde metamorphism.

Because AhS (asteroid 2008 TC_3) as a whole is classified as a polymict ureilite, which does not exhibit evidence of aqueous alteration, it was derived from a parent body that was not the original (CC) parent body of stone 202. Most CC parent bodies are thought to be <100 km diameter[13] and thus would not be sufficiently large to produce the range of P/T conditions represented by the mineral assemblage in AhS 202 (Methods, Supplementary Figure 2). As such, it is our interpretation that the original parent body of AhS 202 was probably an unknown object, potentially Ceres-sized (~640 – 1800 km diameter under the most likely conditions, Methods and Supplementary Figure 3), and more materials like AhS 202 may be present in the Solar System. Furthermore, based on their oxygen isotopic signatures, Allende and AhS 202 are from different CC parent bodies, making this general type of alteration potentially more widespread in the early Solar System than is appreciated from CC meteorites, due to biased sampling[21,22] and/or because amphiboles are present but have been dismissed as “bad” chemical (e.g., EMPA) analyses.

Orbital spectroscopy of asteroids visited by the Hayabusa2 and OSIRIS-REx missions (Ryugu and Bennu, respectively) demonstrates that they are consistent with aqueously altered CC meteorites[23,24]. Mounting spectral evidence suggests that both asteroids differ from most known meteorites in terms of their hydration state[24] and evidence for large-scale, low-temperature hydrothermal processes[25,26]. The OSIRIS-REx results, in particular, have been interpreted as suggesting that Bennu’s surface materials may not be represented by CC meteorites measured on Earth. We are not proposing that AhS 202 is a spectral analogue for Bennu or Ryugu; however, AhS 202 is a serendipitous source of information about early Solar System materials that are not represented by whole meteorites in our collections. The difference between its mineralogy and that of known CC meteorites suggests that unique samples like AhS 202 (and xenoliths in other, non-CC meteorites) could be crucial missing links to understanding the diversity of parent asteroids. This idea will be further supported if missions like Hayabusa2 and OSIRIS-REx return samples that differ from what we have in our collections of meteorites. The differences between xenolith compositions, returned

samples, and those of whole meteorites may be largely an indicator of physical properties that do not readily permit the survival of such materials through the processes of ejection, transit, and entry through Earth's atmosphere, at least not in their original geologic context. Our work ultimately predicts that there are more carbonaceous chondrite materials in the Solar System than are represented by our collections of meteorites.

Methods

Sample.

Almahata Sitta 202 had an original mass of 20.057 g[4]. We were allocated <50 mg from which we prepared a polished mount (area ~8.8 mm^2) and a small chip for bulk oxygen isotope analyses. AhS 202 has a chondritic texture of altered or partially altered chondrules (up to 700 μm diameter) in a completely altered matrix (Fig. 1). The chondrules have thick rims of magnetite with included Fe,Ni sulfides. The interiors of some chondrules contain massive olivine, as well as texturally complex mineral assemblages of amphibole, diopside, serpentine, and other phases. Other chondrules have completely altered interiors. There are also spherules of magnetite (up to ~450 μm diameter) containing inclusions of apatite and Fe,Ni sulfides. The matrix is similar to the alteration assemblages in the chondrules.

Infrared spectroscopy and mineral abundance modeling.

Infrared spectra were measured on the polished mount of AhS 202 using a Thermo Scientific iN10 Fourier transform infrared microscope (μ-FTIR) at Southwest Research Institute in Boulder, CO. This instrument measures reflectance from ~4,000 – 400 cm^{-1} (~2.5 – 25 μm) using a nitrogen-cooled, extended-range, mercury-cadmium-telluride (MCT) detector with a KBr beamsplitter. A spectral map of AhS 202 was collected at 100 $μm^2$/pixel with a size of 22 × 43 pixels (946 spectra), which covered the majority of the sample. Each spectrum is the average of 256 scans or ~1.5 min of integration time at a spectral sampling of ~4 cm^{-1}. Pixels that fell on the edge of the sample or whose spectra were visibly contaminated by fusion crust or epoxy signatures were set to zero, leaving a total of 697 spectra for analysis. Targeted measurements (discrete point spectra) were acquired with the instrument aperture set to various square or rectangular sizes, typically between 20 and 100 μm on a side, designed to isolate minerals of interest. Radiance spectra were ratioed to measurements of a polished gold plate to obtain reflectance, removing instrumental and most atmospheric contributions in the process. The gold plate was measured every 15 minutes during the map acquisition to mitigate any effects of changing instrument or atmospheric conditions. The instrument has a permanently aligned, 15X, 0.7 N.A. (half angle range 20° to 43.5°) visible/IR objective and condenser. This is a sufficiently small solid angle that our reflectance spectra do not suffer from the band broadening effects near the Christiansen feature (CF) observed in biconical systems having large solid angles that include (near-) grazing angles of incidence and collection[27]. This also means that reflectance spectra acquired with this spectrometer can be inverted via Kirchhoff's Law for comparison with spectra acquired in emission, even if it is not a hemispherical measurement[27–29].

The infrared spectra of minerals in mixtures (e.g., meteorites) add linearly in proportion to their abundance; as such we have computed the average spectrum for AhS 202 from the

spectral map acquired on the sample. We then used a non-negative, least squares fitting algorithm[30] to model the modal mineralogy of the average AhS 202 spectrum. The inputs to the model were: 1) the average map spectrum to be modeled, 2) a library containing spectra of a range of likely carbonaceous chondrite phases measured in emission[12] as well as spectra obtained by targeted μ-FTIR measurements on AhS 202 (see below), and 3) the range over which the model should fit the input AhS 202 average spectrum, which was 1300–410 cm^{-1}. The algorithm produces the best-fit spectrum, the phases that comprise the best fit and their fractional abundances, and an RMS error. Because RMS error is partly dependent on the spectral contrast of the measured and modeled spectra, as well as the spectral range of the fit it varies between samples and measurements; for this reason, RMS error is not emphasized in this work and the quality of the spectral fit (e.g., as assessed by the reproduction of measured features, and represented here quantitatively by the residual spectrum) is described instead.

The library we used for the modeling consisted of 72 spectra. Terrestrial phases include coarse particulate (typically 710–1000 μm): phyllosilicates (lizardite, antigorite, chrysotile, cronstedtite, saponite, clinochlore, talc), clino- and orthopyroxenes (enstatite, bronzite, diopside, augite, and hedenbergite), olivines spanning the solid solution series from forsterite (Fo_{90}) to fayalite (Fo_1), amphiboles (tremolite, actinolite, and hornblende), and oxides and hydroxides (magnetite and brucite). Spectra of some phases measured in AhS 202 showed sufficiently different features from their terrestrial counterparts that we also included them in the library. These are: small crystallite[31] olivine, crystallographically-oriented olivine and tremolite, chrysotile, and clinochlore. Following standard practice, we include a blackbody endmember to account for spectral contrast differences[32]; the modeled phase abundances are normalized to 100 vol% to exclude this component. For simplicity, we report the modal mineralogy in the text by mineral group (phyllosilicate, amphibole, olivine, oxide) with the properly propagated uncertainties.

Scanning Electron Microscopy (SEM) and Electron Microprobe Analysis (EMPA).

Secondary electron images (SEI), back-scattered electron images (BEI), elemental X-ray maps, and quantitative electron microprobe analyses (EMPA) were obtained using the JEOL 8530-FE electron microprobe at the Electron Beam Laboratory of the Astromaterials Research and Exploration Science (ARES) Branch, Johnson Space Center (JSC). Quantitative analyses used 15 KeV accelerating potential, with beam current and size depending on the phase(s) being analyzed: 25–30 nA, focused beam (~1 μm diameter) for olivine, pyroxene and magnetite; 10–15 nA, defocused beam (~2–5 μm) for amphibole, serpentine, clinochlore, phosphates, and mixed analyses of matrix phases. Standards used were natural and synthetic minerals, oxides, metals and glasses. Standards for Cl and F were tugtupite and apatite, respectively. Beam-sensitive elements such as Na, F, and Cl were always analyzed first on separate spectrometers. X-ray mapping utilized the Noran System Seven software and Bruker energy dispersive spectrometer (EDS) on the JEOL 8530-FE using 15 KeV accelerating voltage and 30 or 40 nA beam current. Elemental maps were combined into RGB images using ImageJ software.

Transmission Electron Microscopy (TEM).

One electron transparent sample of AhS 202 was prepared from a carefully-selected position on a polished section at the Electron Beam Analytical Facility of the ARES JSC Electron Beam Laboratory using a Quanta 3D FEG Dual-Beam Focused Ion Beam (FIB) instrument equipped with two XEDS detectors for chemical analysis, including spectrum collection and qualitative and quantitative elemental mapping. We cut the FIB section to approximately 100nm thickness. We investigated the mineralogy and mineral textures from the FIB slice using a JEOL 2000FX STEM with a Link EDX image processing system, also at ARES JSC. We calibrated lattice fringe spacing measurements and size scales using a carbon standard.

Amphibole formula calculation and nomenclature.

Supplementary Tables 2 and 3 give EMPA-measured compositions (wt.% and formula assignments) of the average AhS 202 amphibole and four amphiboles from the Arizona State University spectral library[12]. Re-calculated amphibole formulae were used to determine formula site assignments and the amphibole nomenclature (group, subgroup, and species) following the International Mineralogical Association (IMA) 2012 guidelines[33] and using the supplemental spreadsheet from Locock[34], assuming the monoclinic crystal system, 24 anions, and (OH,F,Cl) = 2. The ratio Fe^{3+}/Fetotal was calculated by constraining the sum of cations to be either 13 or 15, and assuming electroneutrality for the entire formula[34]. Based on this analysis, AhS 202 amphibole is tremolite and has the following formula, where "□" denotes a vacancy:

$$(\square_{0.97}Na_{0.03})_{1.0}(Ca_{1.84}, Na_{0.16})_{2.0}\left(Mg_{4.58}, Fe^{2+}_{0.16}, Fe^{3+}_{0.24}, Mn_{0.02}\right)_{5.0}\left(Si_{7.88}Al_{0.04}, Fe^{3+}_{0.08}\right)_{8.0}O_{22}(OH)_{2.0}$$

Constraints on P-T conditions and parent body size.

The anhydrous, major element bulk composition of AhS 202, calculated using modal mineral abundances determined in this work and mineral compositions from EMPA (Supplementary Table 1), is virtually identical (except for a small difference in Mg#) to a terrestrial mantle peridotite composition. This parity means that metamorphic facies and mineral equilibria for terrestrial ultramafic rock[35] can be directly applied to AhS 202. The assemblage serpentine + diopside + tremolite + olivine (± chlorite) is indicative of the greenschist facies, and the equilibrium reaction serpentine + diopside = tremolite + olivine + H_2O can be used to constrain peak P-T conditions[32]. We calculated this curve using Thermocalc[36,37] for the specific mineral compositions in AhS 202 over a pressure range appropriate for small bodies (Supplementary Figure 2). Formation of tremolite (or amphibole in general) is hindered by sluggish kinetics at low pressures and temperatures[38,39], implying that the minimum temperatures at which tremolite is likely to have formed in AhS 202 are 400 – 425 °C, corresponding to 0.5 – 2.0 kbar.

These pressure estimates allow us to constrain the size of the AhS 202 parent asteroid. Supplementary Figure 3 shows calculated depths of derivation, normalized from the surface (0.0) to the core (1.0), vs. asteroid diameter for target pressures of 0.5 kbar and 2.0 kbar, assuming that the asteroid is homogeneous. For each pressure, calculations are shown for

densities of 2.2 g/cm^3 and 3.0 g/cm^3. The former corresponds to the average density of CM (phyllosilicate-rich) chondrites and the latter corresponds to average densities of and CO, CR, and CV (mostly anhydrous) chondrites[40]. Because ~90% of the minerals in AhS 202 are hydrous (phyllosilicates and tremolite), the lower values in this density range may be most appropriate. Minimum asteroid sizes are given by the assumption that the sample is derived from the center of the body (normalized depth of 1.0). More realistically, if the sample is derived from depths corresponding to 20–50% of the radius (normalized depths of 0.2 – 0.5), asteroid diameters in the range ~640 – 1800 km are implied. These sizes are all much larger than inferred for typical CC parent bodies (<100 km) and encompass the size of Ceres (~940 km diameter). We note that the pressures shown in Supplementary Figure 3 are lithostatic pressures, which would correspond to fluid (H_2O) pressure only if there is no open system permeability in the asteroid. If the fluid (H_2O) pressure is less than the lithostatic pressure, even larger parent bodies are required.

Supplementary Material

Refer to Web version on PubMed Central for supplementary material.

Acknowledgements

VEH, CAG, and MEZ are supported by grant 80NSSC19K0507 from NASA's Emerging Worlds program. MEZ was also supported by the Hayabusa2 Participating Scientist Program (NASA). A. Fioretti initially recognized and selected of AhS 202 for analysis, made the mount and collected early SEM observations. We thank J. Filiberto (LPI/USRA) for contributing to scientific discussions. The Lunar and Planetary Institute (LPI) is operated by Universities Space Research Association (USRA) under a cooperative agreement with the Science Mission Directorate of NASA. This is LPI Contribution no. 2546.

References

1. Brearley AJ & Jones RH in Planetary Materials Vol. 36 Reviews in Mineralogy (ed Papike JJ) Ch. 3, 3-001-003-398 (Mineralogical Society of America, 1998).
2. Brearley AJ Disordered biopyriboles, amphibole, and talc in the Allende meteorite: Products of nebular or parent body aqueous alteration? Science 276, 1103–1105 (1997). [PubMed: 9148802]
3. Jenniskens P et al. The impact and recovery of asteroid 2008 TC_3. Nature 458, 485–488 (2009). [PubMed: 19325630]
4. Shaddad MH et al. The recovery of asteroid 2008 TC_3. Meteorit. Planet. Sci 45, 1557–1589, doi:10.1111/j.1945-5100.2010.01116.x (2010).
5. Horstmann M & Bischoff A The Almahata Sitta polymict breccia and the late accretion of asteroid 2008 TC_3. Chem. Erde 74, 149–183 (2014).
6. Goodrich CA et al. Origin and history of ureilitic material in the solar system: The view from asteroid 2008 $TC_3$and the Almahata Sitta meteorite. Meteorit. Planet. Sci 50, 782–809 (2015).
7. Downes H, Mittlefehldt DW, Kita NT & Valley JW Evidence from polymict ureilite meteorites for a disrupted and re-accreted single ureilite parent asteroid gardened by several distinct impactors. Geochim. Cosmochim. Acta 72, 4825–4844 (2008).
8. Patzek M, Pack A, Bischoff A, Visser R & John T Mineralogy of volatile-rich clasts in brecciated meteorites. Meteorit. Planet. Sci 53, 2519–2540 (2018).
9. Goodrich CA et al. Carbonaceous chondrite-like xenoliths in polymict ureilites: A large variety of unique outer solar system materials. Lunar and Planetary Science 50, Abstract #1312 (2019).
10. Fioretti A. A report on 63 newly sampled stones of the Almahata Sitta fall (asteroid 2008 TC3) from the University of Khartoum collection, include a C2 carbonaceous chondrite. Lunar and Planetary Science Conf; 2017. Abstract #1846

11. Goodrich CA et al. The Almahata Sitta polymict ureilite from the University of Khartoum collection: Classification, distribution of clast types in the strewn field, new meteorite types, and implications for the structure of asteroid 2008 TC_3. Lunar and Planetary Science 49, Abstract #1321 (2018).
12. Christensen PR et al. A thermal emission spectral library of rock-forming minerals. J. Geophys. Res 105, 9735–9739 (2000).
13. Brearley AJ in Meteorites and the Early Solar System II (eds Lauretta DS & McSween HY Jr.) 587–624 (University of Arizona Press, 2006).
14. Hamilton VE. Discovery of abundant tremolite in a carbonaceous chondrite fragment from the Almahata Sitta meteorite. Lunar Planet. Sci. Conf.; 2020. 1122
15. Ikeda Y An overview of the research consortium, "Antarctic carbonaceous chondrites with CI affinities, Y-86720, Y-82162, and B-7904". Proceedings NIPR Symposium on Antarctic Meteorites 5, 49–73 (1992).
16. Tonui E et al. Petrographic, chemical and spectroscopic evidence for thermal metamorphism in carbonaceous chondrites I: CI and CM chondrites. Geochim. Cosmochim. Acta 126, 284–306 (2014).
17. Geiger T & Bischoff A Formation of opaque minerals in CK chondrites. Plan. Space Sci 43, 485–498 (1995).
18. Huss GR, Rubin AE & Grossman JN in Meteorites and the Early Solar System II (eds Lauretta DS & McSween HY) 567–586 (The University of Arizona Press, 2006).
19. McCanta M et al. The LaPaz Icefield 04840 meteorite: Mineralogy, metamorphism, and origin of an amphibole- and biotite-bearing R chondrite. Geochmica et Cosmochimica Acta 72, 5757–5780 (2008).
20. Gross J, Treiman AH & Connolly HC Jr. A new subgroup of amphibole-bearing R chondrites: Evidence from the new R-chondrite MIL 11207. Lunar Planet. Sci. Conf., Abstract #2212 (2013).
21. Sears DWG The case for rarity of chondrules and calcium-aluminum-rich inclusions in the early Solar System and some implications for astrophysical models. Astrophys. J 498, 773–778 (1998).
22. Flynn GJ, Consolmagno GJ, Brown P & Macke RJ Physical properties of the stone meteorites: Implications for the properties of their parent bodies. Chem. Erde 78, 269–298 (2018).
23. Hamilton VE et al. Evidence for widespread hydrated minerals on asteroid (101955) Bennu. Nature Astronomy 3, 332 – 340, doi:10.1038/s41550-019-0722-2 (2019).
24. Kitazato K et al. Surface composition of asteroid 162173 Ryugu as observed by the Hayabusa2 NIRS3 instrument. Science 364, 272–275 (2019). [PubMed: 30890589]
25. Simon AA et al. Widespread distribution of carbon-bearing materials on near-Earth asteroid (101955) Bennu. Science, doi:10.1126/science.abc3522 (2020).
26. Kaplan HH et al. Bright carbonate veins on asteroid (101955) Bennu: Implications for aqueous alteration history. Science, doi:10.1126/science.abc3557 (2020).
27. Salisbury JW, D'Aria DM & Jarosewich E Midinfrared (2.5–13.5 μm) reflectance spectra of powdered stony meteorites. Icarus 92, 280–297 (1991).
28. Ruff SW, Christensen PR, Barbera PW & Anderson DL Quantitative thermal emission spectroscopy of minerals: A laboratory technique for measurement and calibration. J. Geophys. Res 102, 14899–14913 (1997).
29. Hamilton VE Spectral classification of ungrouped carbonaceous chondrites I: Data collection and processing. Lunar and Planetary Science XLIX, Abstract #1759 (2018).
30. Rogers AD & Aharonson O Mineralogical composition of sands in Meridiani Planum determined from Mars Exploration Rover data and comparison to orbital measurements. J. Geophys. Res 113, E06S14, doi:10.1029/2007JE002995 (2008).
31. Hamilton VE, Haberle CW & Mayerhöfer TG Effects of small crystallite size on the thermal infrared (vibrational) spectra of minerals. Am. Mineral (in press).
32. Hamilton VE, Christensen PR & McSween HY Jr. Determination of Martian meteorite lithologies and mineralogies using vibrational spectroscopy. J. Geophys. Res 102, 25593 – 25603 (1997).
33. Hawthorne F et al. IMA report, nomenclature of the amphibole supergroup. Am. Mineral 97, 2031–2048 (2012).

34. Locock AJ An Excel spreadsheet to classify chemical analyses of amphiboles following the IMA 2012 recommendations. Computers and Geosciences 62, 1–11 (2014).

35. Bucher K & Grapes R Petrogenesis of Metamorphic Rocks. 8 edn, (Springer-Verlag, 2011).

36. Powell R & Holland T An internally consistent dataset with uncertainties and correlations: 3. Applications to geobarometry, worked examples and a computer program. J. Metamorph. Geol 6, 173–204 (1988).

37. Holland T & Powell R An improved and extended internally consistent thermodynamic dtaset for phases of petrological interest, involving an new equation of state for solids. J. Metamorph. Geol 29, 333–383 (2011).

38. Pawley AR, Graham CM & Navrotsky A Tremolite-richterite amphiboles: Synthesis, compositional and structural characterization, and thermochemistry. Am. Mineral 78, 23–35 (1993).

39. Maresch WV & Czank M Crystal chemistry, growth kinetics and phase relationships of structurally disordered (Mn2+,Mg)-amphiboles. Fortschr. Mineral 66, 69–121 (1988).

40. Macke RJ, Consolmagno GJ & Britt DT Density, porosity, and magnetic susceptibility of carbonaceous chondrites. Meteorit. Planet. Sci 46, 1842–1862 (2011).

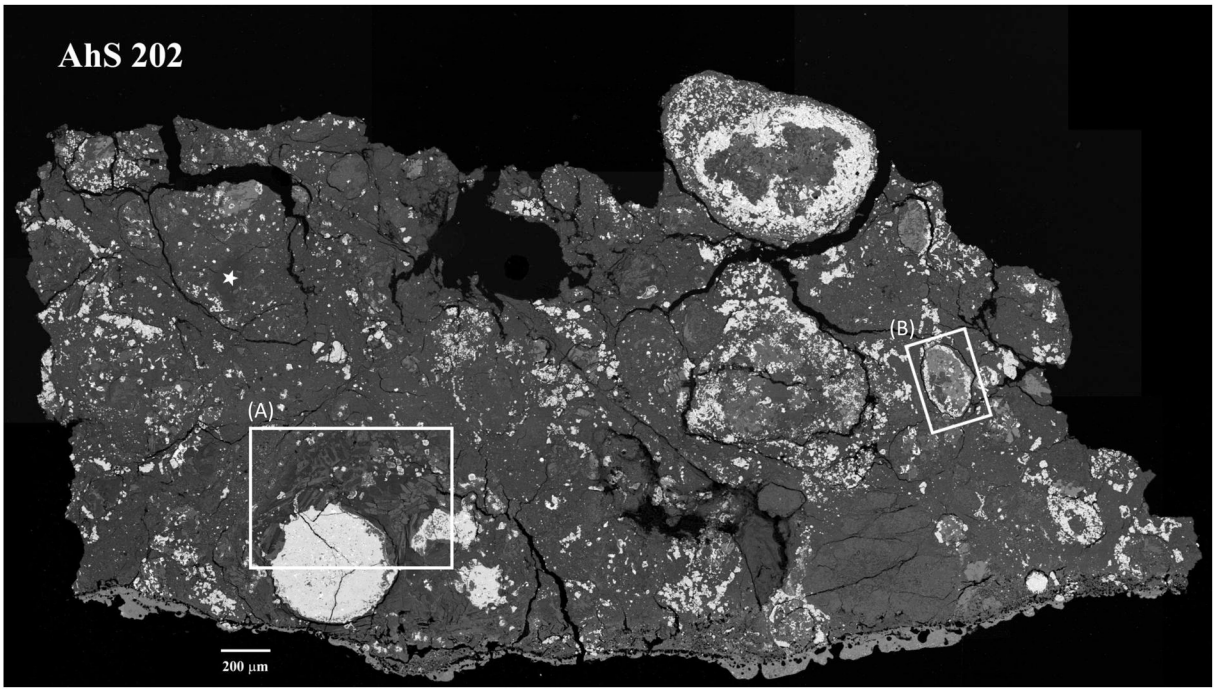

Fig. 1.

Backscattered electron (atomic number contrast) image of AhS 202. Brighter areas represent higher atomic numbers. AhS 202 contains altered chondrules (commonly rimmed by magnetite and Fe-Ni sulfides) in a completely altered matrix. The white boxes (labeled A and B) delineate the areas shown in Fig. 3. The white star denotes the approximate location of the FIB-TEM analysis shown in Supplementary Figure 1.

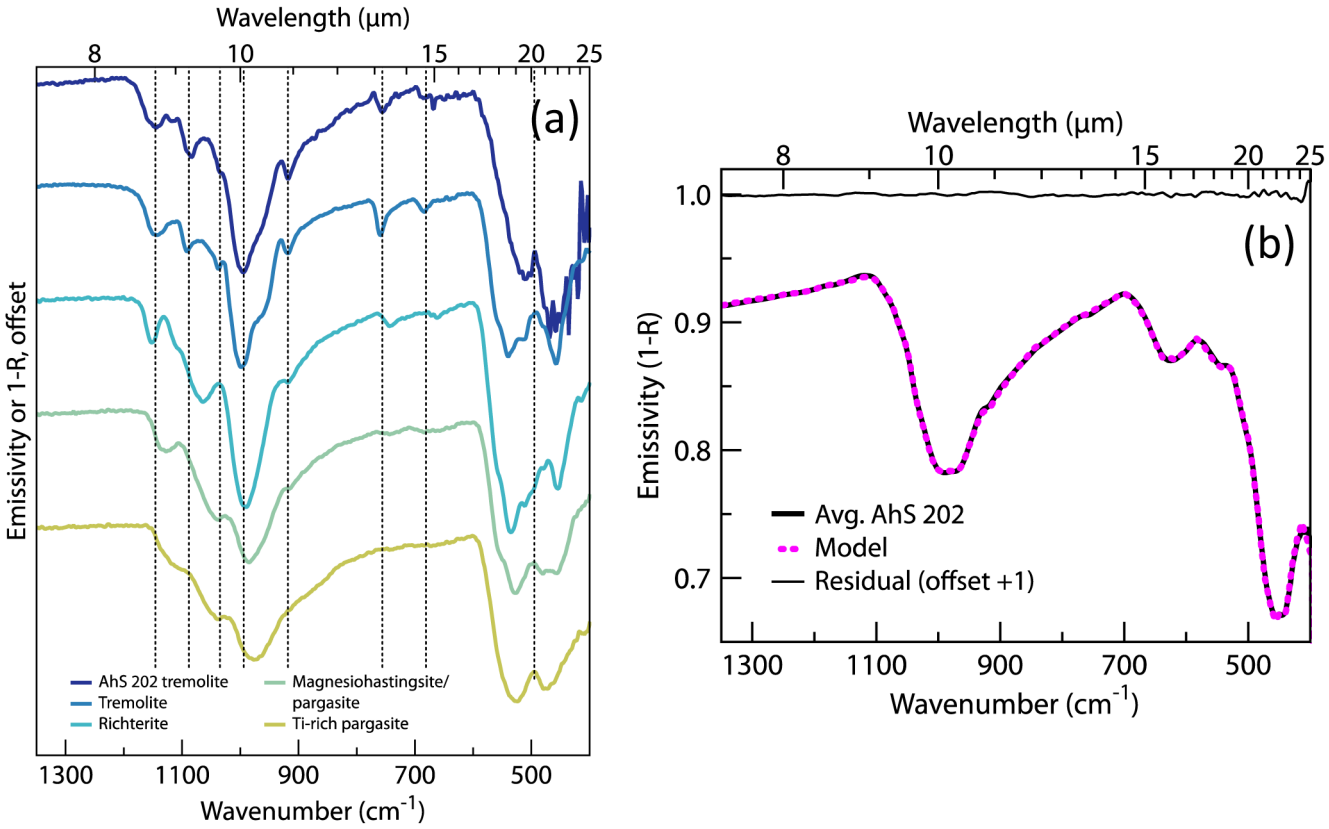

Fig. 2.

Infrared spectra from AhS 202, terrestrial amphiboles, and model fit. (a) Infrared spectrum of tremolite in AhS 202 compared to terrestrial calcic amphiboles (bulk chemistries are shown in Supplementary Tables 2 and 3). Vertical lines indicate positions of key features in AhS 202 tremolite spectrum, which is the average of 256 scans; increased noise at <~475 cm $^{-1}$ is attributable to fall-off in detector sensitivity. (b) Infrared (whole-rock) measured spectrum of AhS 202, modeled spectrum, and residual (measured-modeled). The low residual indicates that the model reproduces all diagnostic features and that the resultant modal mineralogy is accurate to within the stated uncertainty. The AhS 202 spectrum is the average of 163 map spectra acquired at 256 scans each and represents a factor of 12.8 improvement in SNR over the spectrum in Fig. 2a. See Methods for additional details.

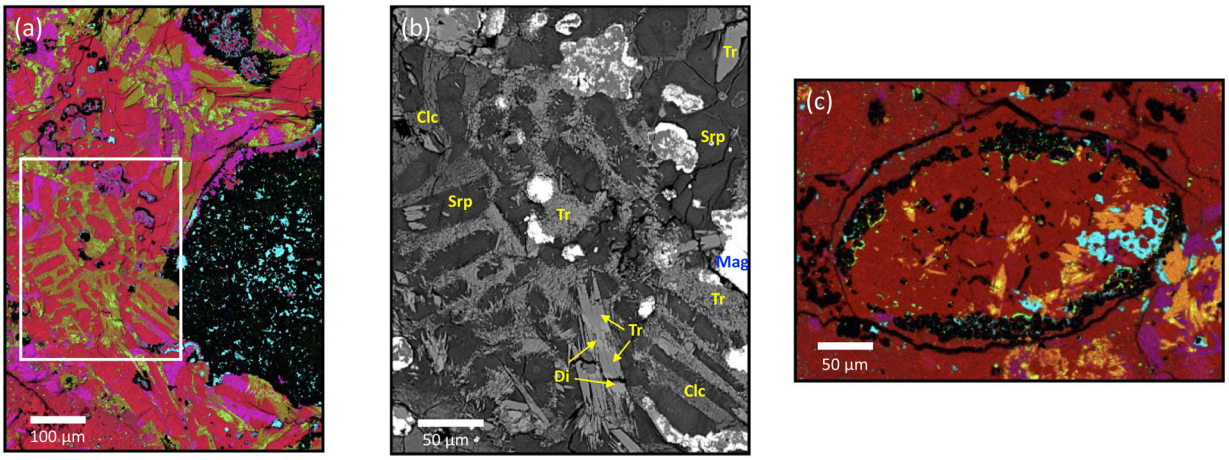

Fig. 3.

X-ray elemental and backscattered electron (BSE) images of minerals and textures in AhS 202. (a) Colorized X-ray image (Red=Mg, Green=Ca, Blue=Al, Cyan=S) of a tremolite-bearing area adjacent to a large magnetite spherule (ref. Fig. 1). Tremolite is darker yellow-green, diopside is brighter yellow-green, serpentine is red, clinochlore is magenta, magnetite is black, and sulfide is cyan; the white box delineates the area shown in (b). (b) High-resolution BSE image showing textural details of area in Fig. 3a. Serpentine (Srp) is dark grey, clinochlore (Clc) is medium grey, tremolite (Tr) is medium-light grey, diopside (Di) is lightest grey, and magnetite (Mag) is bright white, as are sulfides (not identified). Arrows denote region where tremolite is replacing diopside, which largely only remains in the core of the grain. (c) Colorized X-ray image (Red=Si, Green=Ca, Blue=Al, Cyan=S) of a tremolite-bearing area in and around a small chondrule (ref. Fig. 1). Tremolite (orange) is replacing diopside (bright, yellow), which is most commonly present in the cores of elongate grains.